Computer-Aided Design, Synthesis and Validation of 2-Phenylquinazolinone Fragments as CDK9 Inhibitors with Anti-HIV-1 Tat-Mediated Transcription Activity

13 AUTHORS, INCLUDING:

Nunzio Iraci
Università degli Studi di Perugia
40 PUBLICATIONS **595** CITATIONS

Stefano Sabatini
Università degli Studi di Perugia
52 PUBLICATIONS **656** CITATIONS

Giuseppe Manfroni
Università degli Studi di Perugia
42 PUBLICATIONS **429** CITATIONS

Oriana Tabarrini
Università degli Studi di Perugia
93 PUBLICATIONS **1,245** CITATIONS

Computer-Aided Design, Synthesis and Validation of 2-Phenylquinazolinone Fragments as CDK9 Inhibitors with Anti-HIV-1 Tat-Mediated Transcription Activity

Luca Sancineto,[a] Nunzio Iraci,[a] Serena Massari,[a] Vanessa Attanasio,[a, b] Gianmarco Corazza,[b] Maria Letizia Barreca,[a] Stefano Sabatini,[a] Giuseppe Manfroni,[a] Nilla Roberta Avanzi,[c] Violetta Cecchetti,[a] Christophe Pannecouque,[d] Alessandro Marcello,*[b] and Oriana Tabarrini*[a]

The activity of the cyclin-dependent kinase 9 (CDK9) is critical for HIV-1 Tat-mediated transcription and represents a promising target for antiviral therapy. Here we present computational studies that, along with preliminary synthetic efforts, allowed us to identify and characterize a new class of nontoxic anti-CDK9 chemotypes based on the 2-phenylquinazolinone scaffold. Inhibition of CDK9 translated into the ability to interfere selectively with Tat-mediated transactivation of the viral promoter and in the inhibition of HIV-1 reactivation from latently infected cells, with the most potent derivative **37** (2-(4-amino-phenyl)-7-chloroquinazolin-4(3H)-one) showing an IC_{50} value of 4.0 μm. Because the herein reported 2-phenylquinazolinones are merely fragments, they are largely optimizable, paving the way to derivatives with improved potency.

Introduction

The human immunodeficiency virus type 1 (HIV-1) is a retrovirus that requires integration into host chromatin to transcribe its genome for productive infection. HIV-1 infection can be effectively controlled by combination antiretroviral therapy (cART), which improves the quality of life in infected individuals but unfortunately fails to completely eradicate the virus even after decades of treatment.[1,2] Viral reservoirs persist during therapy mostly in memory T cells that harbor a transcriptionally silent integrated provirus.[3] Reactivation from latency critically depends on the viral transactivator protein Tat, that acts like a molecular switch between silent and productive transcription.[4] In the absence of Tat, basal transcription from the long terminal repeat (LTR) ultimately causes RNA polymerase II (RNAPII) to pause after synthesis of a short RNA that includes the Tat responsive element (TAR). The negative elongation factors are recruited to induce pausing of RNAPII on the promoter.[5] Tat counteracts RNAPII pausing by binding TAR and recruiting the positive transcription elongation factor b (P-TEFb) complex. The core constituents of P-TEFb are cyclin T1 (CycT1) and the cyclin-dependent kinase 9 (CDK9) that phosphorylates the RNAPII carboxy terminal domain (CTD) and the negative transcription elongation factors, licensing RNAPII for productive elongation.[6]

Tat-mediated HIV-1 transcription represents a valid target to prevent HIV-1 replication and its re-emergence from latency.[7] Developing chemicals that target P-TEFb, which is a key element in Tat-mediated activation of the HIV-1 LTR promoter but is not needed for cell survival, could be a compelling strategy.[8] Such "indirect antiviral drugs" should not select for mutant viruses resistant to treatment and should be active even against mutant viruses eventually escaping current therapies. In addition, they may also be active against other viruses, since replication of unrelated viruses often requires the same cellular factors.

Several experimental evidences have already validated CDK9 as a druggable component of the P-TEFb complex and confirmed that host and viral transcription might be differently sensitive to P-TEFb inhibition,[6,9–15] thus providing a rationale for targeting P-TEFb as a potential strategy for developing new anti-HIV-1 therapeutics. The majority of CDK inhibitors were firstly identified by retrospectively screening anticancer agents towards a panel of CDKs. Among them, flavopiridol (**1**; Figure 1) emerged as one of the most potent, but showed only a 10-fold preference for CDK9[12,16] and a certain degree of cytotoxicity.[17] Recently, few example of more potent and se-

[a] Dr. L. Sancineto,+ Dr. N. Iraci,+ Dr. S. Massari, Dr. V. Attanasio, Dr. M. L. Barreca, Dr. S. Sabatini, Dr. G. Manfroni, Prof. V. Cecchetti, Dr. O. Tabarrini
Department of Chemistry and Technology of Drugs
University of Perugia, 06123 Perugia (Italy)
E-mail: oriana.tabarrini@unipg.it

[b] Dr. V. Attanasio, Dr. G. Corazza, Prof. A. Marcello
Molecular Virology Group, International Centre for Genetic Engineering and Biotechnology (ICGEB), 34012 Trieste (Italy)
E-mail: marcello@icgeb.org

[c] Dr. N. R. Avanzi
Nerviano Medical Sciences, 20014 Nerviano (Italy)

[d] Prof. C. Pannecouque
Rega Institute for Medical Research
Katholieke Universiteit Leuven, 3000 Leuven (Belgium)

[+] These authors contributed equally to this work.

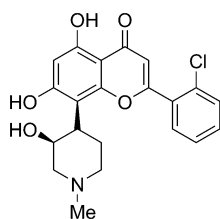Supporting information for this article is available on the WWW under http://dx.doi.org/10.1002/cmdc.201300287.

Figure 1. Flavopiridol (**1**).

lective CDK9 inhibitors were reported for their anti-HIV-1 activity.[18–21]

To identify novel anti-CDK9 chemotypes and as a part of our continuous search for Tat-mediated transcription inhibitors,[22,23] we have implemented a structure-based drug discovery (SBDD) strategy exploiting the structural information of P-TEFb in complex with **1**.[24] We herein report the computational studies that, along with a first round of structural optimization (Figure 2), led to the identification of the 2-phenylquinazolinone scaffold for the development of CDK9 inhibitors as promising anti-HIV-1 agents.

fragment scaffolds were visually inspected, taking into account, beside the docking scores and the desired pharmacophore features, their synthetic accessibility. Quinazoline fragment **2** satisfied the wanted requirements (Figure 2; XP GScore = −8.3207, Rank = 8) and was then selected for the enzymatic assay. Fragment **2** in its Glide-predicted binding pose within the ATP binding site overlapped to the experimental position of the 4H-chromen-4-one scaffold of **1** (Figure 3), making hydrophobic interaction mainly with residues Val33, Ala46, Val79, Phe103, Leu156 and Ala166. Notably, **2** was able to establish two hydrogen bonds with the backbone of Cys106 by its amide moiety, whereas the 4H-chromen-4-one moiety was engaged in only one hydrogen bond between its carbonyl oxygen and the backbone NH of Cys106.

The anti-CDK9 kinase activity evaluation showed that **2** was able to inhibit CDK9 activity to about 50 % albeit at a high concentration (500 μm, see figure S1 in the Supporting Information). With the aim to build an ad hoc fragment-based library, the active fragment **2** was chosen as scaffold. In particular, it was used as a query in a substructure search performed on the molecules website,[26] looking for commercially available molecules based on such a scaffold. This search resulted in a 13 102-membered library that was screened in silico along with the Gold (205 659 compounds) and Platinum (118 763 compounds) collections from the vendor Asinex[27] and our in-house database (about 1000 compounds). The compound collections were screened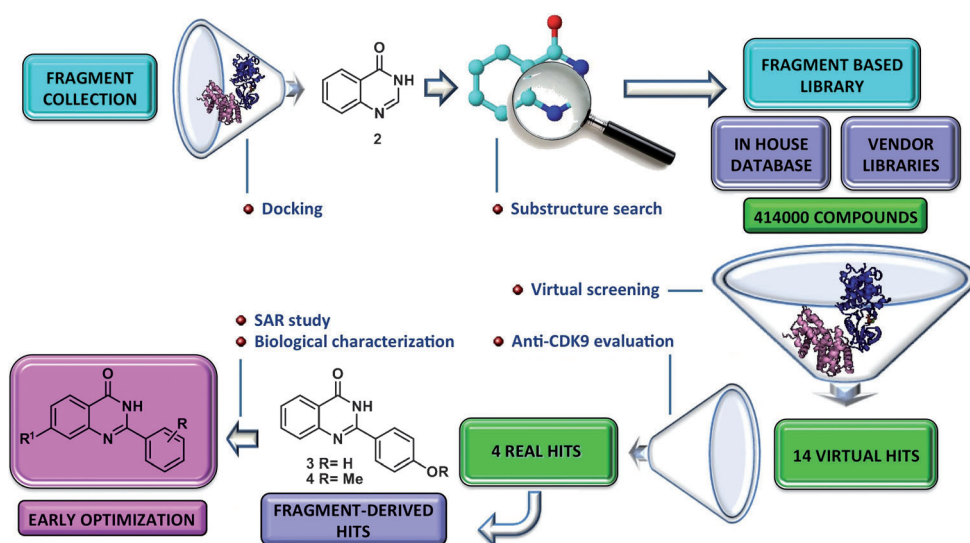 in silico using as target the crystallographic structure of human CDK9/CycT1 in complex with **1**[24] by means of the Glide software, and employing Glide high-throughput virtual screening (HTVS), standard precision (SP) and extra precision (XP) scoring functions in three serial steps to increase the screening speed. Fourteen molecules were selected as "virtual hits" (see table S1) and subsequently submitted to the anti-CDK9 assay at 50 μm concentration. Four derivatives showed the ability to inhibit the kinase with an inhibition percentage ≥ 50 % (see table S1). Among them, 2-phenylquinazolinones **3** and **4** (Figure 2), mined from the fragment-based library, were selected for further studies. Their successive anti-kinase evaluation, carried out at lower concentrations, showed an IC50 value of 51.5 and 50.7 μm for derivatives **3** and **4**, respectively (see figures S2–S4). These compounds were also tested for their cytotoxicity in HeLa cells, where they were nontoxic up to 300 μm.

The tenfold increased anti-CDK9 activity with respect to fragment **2**, coupled with the lack of cytotoxicity, reinforced the

Figure 2. Drug discovery workflow.

Results and Discussion

Hit generation

First of all, test docking calculations using flavopiridol (**1**) were carried out to validate the docking protocol. The ligand was thus extracted from the corresponding P-TEFb complex and then docked back into the active site of the enzyme crystal structure, with the aim of comparing experimental and predicted binding modes and evaluate the program performance. The best docking pose of **1** (selected on the basis of the highest GlideScore: −13.17) agreed well with the experimental binding mode of **1**, with a root-mean square deviation (RMSD) value of 0.6747. To increase the probability of finding synthetically feasible inhibitors, we started our SBDD building an ad hoc fragment-based library to be screened in parallel with two commercial libraries and our in house database. To this end, a first docking-based virtual screening was carried out on the rule-of-three-compliant[25] 441-membered Glide fragment library (Schrödinger, MW range 32–226 Da). The best scoring
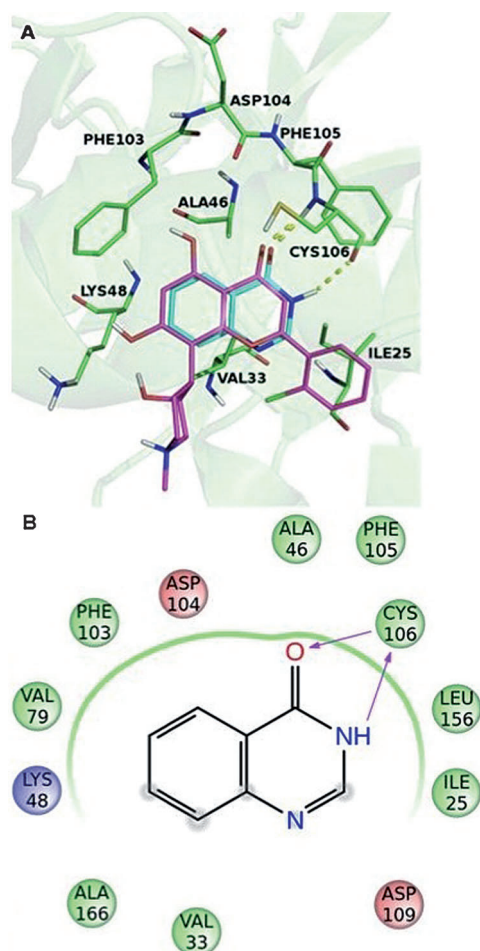
Figure 3. A) Predicted binding mode of fragment **2** (cyan sticks) into the ATP binding site (green sticks and cartoons). Experimental position of **1** is depicted in magenta sticks as reference. Intermolecular hydrogen bonds are shown as yellow dashed lines. B) Schematic representation of the interactions between **2** and CDK9. CDK9 residues lying within a distance of 4 Å from the docked ligand are shown and color coded as follows: green, hydrophobic; red, acidic; purple, basic.

validity of the quinazolinone scaffold as a new chemotype worthy of further optimization.

Hit optimization

With the aim to improve potency and to collect preliminary structure–activity relationship (SAR) information, a two-step optimization study was performed, synthesizing an enlarged series of quinazolinones (**5–41**, Table 1) by combining different medicinal chemistry approaches.

Starting from hit compounds **3** and **4**, the main efforts were initially focused on the phenyl ring at the C-2 position of the quinazolin-4(3*H*)-one scaffold. In particular, the *p*-hydroxy and *p*-methoxy groups were shifted to *ortho* (**5** and **6**) and *meta* (**7** and **8**) positions, respectively, whereas a series of different *p*-*O*-alkylated compounds were realized replacing the methyl with linear (**9** and **10**), as well as branched (**11** and **12**) alkyl chains. The *para* substituent was

then removed (**13**) as well as replaced with a chlorine atom (**14**). The *o*-chlorine and *p*-amino derivatives **15** and **16** were also prepared as suggested by free energy perturbations (FEP)[28] calculations (see table S2). In a more incisive structural modification, an imidazole ring replaced the 2-phenyl ring in compound **17**.

In a parallel approach, in silico combinatorial experiments were carried out to thoroughly explore the binding pocket area around the 2-phenyl moiety. According to the synthetic pathway used to obtain the quinazolinone derivatives (Scheme 1), a combinatorial library was built using the Combi-Glide software.[29] In particular, a substructure search was performed on the entire Sigma–Aldrich database, looking for all the commercially available benzaldehydes. All the mined molecules were then reacted in silico with isatoic anhydride, thus enumerating a combinatorial library (324 compounds) that was screened by automated molecular docking. The docking poses were then visually inspected taking into account, besides the docking score and the required pharmacophore features, the costs of the reactants. This approach resulted in the identification of potentially active, low cost, and easily synthesizable compounds. Among them, quinazolinones **18–26** were selected to be synthesized and tested (Table 1, see docking scores and ranking in table S3).

The anti-CDK9 activity of compounds **5–26** (Table 1) inspired the design of further analogues (**27–41**). In particular, starting from **16**, the *p*-amino group was moved to the *meta* and *ortho* positions giving derivatives **27** and **28**, respectively; the corresponding nitro intermediates **29–31** were also tested. The *p*-amino group was decorated with alkyl and cycloalkyl substituents as in compounds **32–34**.

A few modifications involved the quinazolinone nucleus. In particular, 7-chloro derivatives **35–38** were synthesized following the predictions of FEP simulations (see table S2), whereas N1—C2 saturated quinazolinones **39–41** were included in the kinase assay to acquire preliminary structural information about the importance of the pyrimidine ring.

Chemistry

Various procedures for the synthesis of the quinazolinone scaffold are known.[30] Most of the quinazolinones herein reported, **5**,[31] **6**,[32] **8**,[33] **9–12**, **13**,[34] **14**,[34] **15**,[35] **16**,[36] **17–19**, **20**,[37] **21**,[38] **22**, **23**, **32**,[35] **33**,[39] **34**,[38] **35**,[40] and **36**, were synthesized according to the one-pot multicomponent reaction proposed by Bhat and colleagues in 2004,[34] as outlined in Scheme 1.
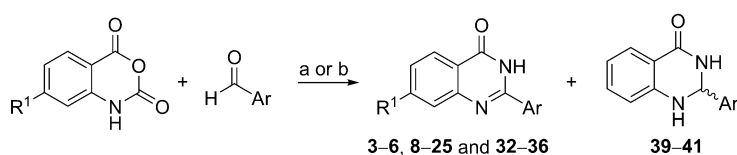
Scheme 1. Synthesis of quinazolinone derivatives **3–6**, **8–25** and **32–36**. For R^1 and Ar, see Table 1. *Reagents and conditions*: a) NH$_4$OAc, I$_2$, KOH, DMF, 85 °C; b) NH$_4$OAc, Yb(OTf)$_3$, DMSO, 90 °C, 4 h, 40–61 %.

Table 1. Structure of quinazolinones synthesized in this study and CDK9 inhibitory activity.[a]

Compd	Ar	Inhibition [%][a]	Compd	Ar	Inhibition [%][a]
3	(4-OH phenyl)	62	19	(pyridin-2-yl–phenyl)	26
4	(4-OMe phenyl)	55	20	(OMe, Br)	43
5	(2-OH phenyl, HO)	38	21	(piperidin-1-yl–phenyl, N)	8
6	(2-OMe phenyl, MeO)	54	22	(naphthalenyl, OH)	0
7	(3-OH phenyl)	31	23	(indazolyl, N–H)	73
8	(3-OMe phenyl)	24	24	(N(Me)CH₂CH₂OH, OH, Me)	73
9	(4-propoxy phenyl)	43	25	(isoquinolinyl, N)	17
10	(4-ethoxy phenyl)	54	26	(HO, OH, OH)	70
11	(4-isopropoxy phenyl)	32	27	(3-NH₂ phenyl)	52
12	(4-isopentoxy phenyl)	55	28	(2-NH₂ phenyl, H₂N)	25
13	(phenyl)	55	29	(4-NO₂ phenyl)	0
14	(4-Cl phenyl)	2	30	(3-NO₂ phenyl)	10
15	(2-Cl phenyl)	42	31	(2-NO₂ phenyl, O₂N)	0
16	(4-NH₂ phenyl)	70	32	(NMe₂, Me/Me)	41

The same procedure was also adopted to resynthesize compounds **3** and **4**.[34]

The reaction of the appropriate isatoic anhydride, selected aryl aldehydes and ammonium acetate in the presence of iodine and potassium hydroxide in dry *N,N*-dimethylformamide (DMF) directly gave the target compounds. Among the employed aldehydes, 4-ethoxy-,[41] 4-propoxy-,[41] 4-isopropoxy-,[42] and 4-isopentoxy- (**42**) benzaldehydes were prepared according to the literature through the alkylation of 4-hydroxybenzaldehyde with the appropriate alkyl iodide in the presence of potassium carbonate, in acetonitrile at reflux (not shown). When the 2-chlorobenzaldehyde was employed, besides the target compound **15** (47 % yield), the N1–C2 dihydro intermediate **39**[35] was also obtained. The sole N1–C2 dihydro derivative **40** was instead obtained when 4-[(2-hydroxyethyl)-(methyl)amino]benzaldehyde was used. Compound **7**[33] was obtained by the demethylation of its methoxy analogue **8** using 48 % hydrogen bromide (not shown).

For the preparation of **24** and **25**, the above described procedure was slightly modified by using ytterbium trifluoromethansulfonate (Yb(OTf)₃) as promoting agent and replacing DMF with dimethyl sulfoxide (DMSO), which also works as mild oxidizing agent.[43] By synthesizing compound **25**, N1–C2 dihydro derivative **41** was also obtained.

In an alternative procedure (Scheme 2), the anthranilamide replaced the isatoic anhydride as starting material. In particular, the reaction of appropriate anthranilamide with nitrobenzoyl chloride in the presence of triethylamine gave intermediates **43**,[44] **44**, **45**,[45] and **46**[46] which were cyclized using potassium *tert*-butoxide in *tert*-butanol giving nitro derivatives **29–31**[46] and **38**.[47] The amino derivatives **27**,[46] **28**,[46] and **37** were obtained by catalytic reduction of corresponding nitro intermediates **30**, **31**, and **38**. Derivative **26** was directly prepared by reacting anthranilamide with trihydroxybenzaldehyde using *p*-toluenesulfonic acid (pTsOH) as catalyst under reflux of methanol.

Biological results

All synthesized compounds were initially tested for their ability to inhibit CDK9 activity at a concentration of 50 μm. The resynthesized compounds **3** and **4**, included in the biological evaluation, showed the same activity of the commercial counterparts. As shown in Table 1, most of the compounds were able to inhibit the enzyme although with different degrees of inhibition.

Although a robust SAR cannot be delineated on the basis of the percentage of inhibition, some clues may emerge by comparing these data with those of the hit compounds **3** and **4**. The substituent at the

Table 1. (Continued)

Compd	Ar	Inhibition [%][a]	Compd	Ar	Inhibition [%][a]
17	(4-methylimidazole)	0	33	(4-methyl-N,N-diethylaniline)	10
18	(3-chloro-2-hydroxy-6-methoxytoluene)	16	34	(4-methylphenyl morpholine)	29
35	(4-methoxytoluene)	52	37	(4-aminotoluene)	70
36	(N-methyl-N-(2-hydroxyethyl)-4-methylaniline)	4	38	(4-nitrotoluene)	0
39	(2-chlorophenyl)	1	41	(isoquinoline)	41
40	(N-methyl-N-(2-hydroxyethyl)aniline)	57			

[a] CDK9 kinase activity was measured in vitro on a recombinant GST-CTD substrate as described previously,[74,75] using 50 μM concentration of the compounds.

Scheme 2. Synthesis of quinazolinone derivatives **26–31**, **37**, **38** and **43–46**. *Reagents and conditions*: a) Et₃N, THF, RT, 6 h, 71%; b) *tert*-butanol, potassium *tert*-butoxide, RT, 24 h, 70%; c) H₂, Raney Ni, DMF, RT, 2 h, 60%; d) pTsOH, 2,3,4-trihydroxybenzaldehyde, MeOH, reflux, 5 h, 43%.

para position of the 2-phenyl ring did not seem to be essential, since compound **13** showed similar activity as compared to the hit compounds. However, when present, the amino group was beneficial (**16**), in line with the FEP predictions made for the *para* position (see table S2). The presence of the *p*-chlorine atom was detrimental (**14**, 2% inhibitory activity), but its FEP-guided (see table S2) shifting to the *ortho* position permitted some activity to be recovered (**15**, 42% inhibitory activity). The addition of a further aromatic ring (**19**) as well as the fusion of the phenyl moiety between its *ortho* and *meta* position with an additional aromatic ring (**22** and **25**) were clearly unfruitful. The lengthening of the methoxy group characterizing hit **4** (as in **9–12**) was tolerated with the only exception of **11** (32% of inhibitory activity). The nitro group was absolutely not allowed in any position of the phenyl ring (see data for **29–31**, and **38**). Concerning the hydroxy and methoxy regioisomers of **3** and **4** (**5–8**), only *o*-methoxy derivative **6** maintained the same activity as the hit compounds. Contrasting results were obtained when assaying dihydroquinazolinone derivatives **39–41**, with compound **39** lacking any ability to inhibit CDK9. Analogously, the addition of a chlorine atom at the C-7 position of active quinazolinones **4**, **16** and **24** gave very different results; high inhibition was maintained by **37**, the 7-chloro analogue of amino derivative **16**.

In summary, the assessment of the anti-CDK9 activity of the whole set of synthesized compounds resulted in the identification of new active derivatives, confirming the 2-phenylquinazolinone as a suitable scaffold for CDK9 inhibitors. Setting a 70% inhibition of kinase activity as hit selection criterion, compounds **16**, **23**, **24**, **26**, and **37**, emerged as the most promising. With the exception of **26**, all of the compounds are structurally characterized by a nitrogen atom at the *para* position of the 2-phenyl ring, as a primary amino group (**16** and **37**), *N,N*-dialkylated (**24**), or embedded in a pyrazole ring (**23**).

For these derivatives, an in-depth biological evaluation was carried out to determine IC₅₀ values, cytotoxicity, and the ability to inhibit Tat-mediated transcription, using **1** as reference compound.

The anti-kinase activity evaluated in serial dilutions showed that all five selected compounds are able to fully inhibit CDK9 in a dose-dependent fashion with IC₅₀ values in the low micromolar range (Table 2): 9.91 μM (**23**), 10.12 μM (**24**), 12.18 μM (**16**), 15.60 μM (**26**), and 26.20 μM

Table 2. Anti-CDK9 activity and anti-HIV-1 activity on acutely (MT-4) and latently (OM-10.1) infected cells of selected 2-phenylquinazolinones.

Compd	CDK9 IC$_{50}$ [μM][a]	MT4 cells IC$_{50}$ [μM][b,d]	CC$_{50}$ [μM][c,d]	SI[e]	OM-10.1 cells IC$_{50}$ [μM][d,f]	CC$_{50}$ [μM][c,d]	SI[e]
16	12.18 (0.67)	>238.1	238.1±9.7	<1	11.8±1.7	338.8±46.4	29
23	9.91 (0.18)	>42.6	42.6±4.2	<1	≥19.1	76.1±19.8	≤4
24	10.12 (0.36)	>42.2	42.2±2.2	<1	14.0±3.4	154.4±9.9	11
26	15.60 (0.04)	>9.2	9.2±1.5	<1	>51.0	51.0±6.8	<1
37	26.20 (0.13)	>170	>170	<1	4.0±0.7	344.9±47.4	86
1	0.015 (0.18)	>0.27	0.27±0.02	<1	0.003±0.0007	0.18±0.01	60

[a] The CDK9 kinase activity was measured in vitro on recombinant GST-CTD substrate as described previously;[73,74] standard errors are shown in brackets. [b] IC$_{50}$: concentration of compound required to achieve 50% protection of MT-4 cells from HIV-1 induced cytopathogenicity, as determined by the MTT method. [c] CC$_{50}$: concentration of compound that reduces the viability of mock-infected cells by 50%, as determined by the MTT method. [d] All data represent mean values ± standard deviations for at least two separate experiments. [e] Selectivity index (SI): ratio of CC$_{50}$/IC$_{50}$. [f] IC$_{50}$: concentration of compound required to achieve 50% reduction of p24 production in HIV-1 infected cells.

(**37**). Thus, compared to those of the hit compounds **3** and **4** (IC$_{50}$≈50 μM), the inhibitory activity of the new derivatives was improved two- to fivefold, and notably, the ligand efficacy (LE) was fully retained and in some cases slightly increased (**4**: LE=0.31; **16**: LE=0.37). However, the compounds were less active than **1**, which, assayed in parallel, inhibited CDK9 with an IC$_{50}$ value of 0.015 μM.

At this point, the cytotoxicity was evaluated in HeLa cells, and only derivative **26** was toxic >100 μM, whereas for all the other derivatives no apparent cytotoxicity was observed even at the highest assayed concentration of 500 μM. It is worth noting that **1** showed a 50% reduction of cell viability at 1 μM (see figure S5).

The five selected quinazolinones were then tested for their ability to inhibit Tat transactivation in order to evaluate whether the in vitro anti-CDK9 activity is preserved and still holds in a whole cell context. The Tat-mediated transcription assay was performed on HeLa cells carrying an LTR-luciferase reporter and using **1** as the positive control. With the only exception of derivative **16**, all of the tested compounds inhibited the transactivation at 50 μM with **37** being the most active, also inhibiting the transactivation at 10 μM (Figure 4).

A constitutive transcription assay was then performed in order to assess whether the anti-transactivation activity could be ascribed to a genuine inhibition of P-TEFb. To this end, HeLa cells were transfected with a plasmid where expression of the reporter *Renilla* gene is driven by the constitutive CMV promoter. No significant activity on the basal transcription was displayed by incubating the cells with our best inhibitor **37**, suggesting a promising target selectivity (Figure 5).

Finally, although the anti-CDK9 activity was not very high and the inhibition of Tat-mediated tran-

scription was observed only at high concentrations, compounds **16**, **23**, **24**, **26**, and **37**, were assayed for their anti-HIV-1 activity on both acutely and latently infected cells (Table 2), none of the tested compounds showed antiviral activity in acutely infected MT-4 cells, where no relevant cytotoxicity was observed with the exception of compound **26**, which displayed some cytotoxicity (CC$_{50}$= 9.2 μM) in agreement to what was observed in HeLa cells. Conversely, in a model of latently HIV-1-infected promyelocytic cells (OM-10.1), where the virus is transcriptionally silent unless stimulated with phorbol myristate acetate (PMA), compounds **16**, **24** and **37** showed good antiviral activities with IC$_{50}$ values in the low micromolar range at concentrations that were far below the observed cytotoxicity. The best inhibitory activity was obtained by **37** with an IC$_{50}$ value of 4.0 μM, which, coupled with a CC$_{50}$ value of 345 μM, led to a selectivity index (SI) of 86.
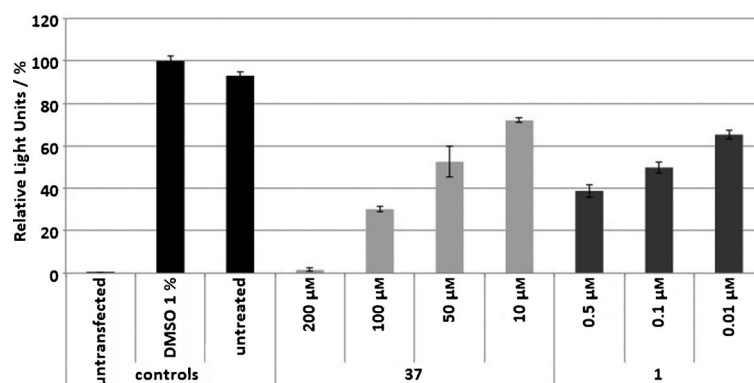

Figure 4. HIV-1 LTR transactivation assay. HeLa LTR-luciferase were activated with Tat at suboptimal doses and treated with increasing concentrations of **37** as described previously.[73] The Firefly luciferase assay was performed on cell lysates 24 h after treatment following standard procedures (Promega) and analyzed with a plate reader (Wallac, PerkinElmer). DMSO, vehicle control; **1**, flavopiridol. Luminescence intensities represented as percentages.
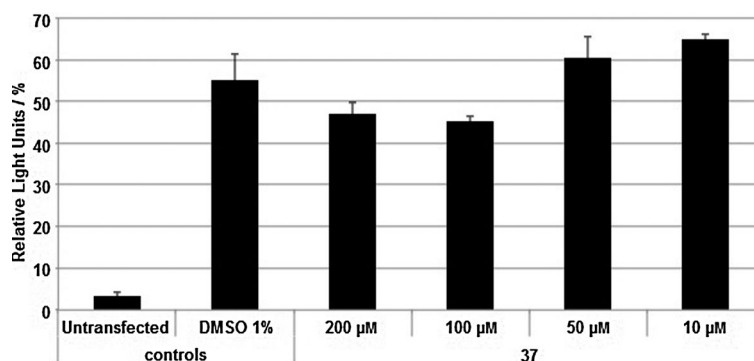

Figure 5. Constitutive transcription assay. HeLa cells were transfected with plasmid pCMV-*Renilla* and treated with increasing concentrations of compound **37**. The *Renilla* luciferase assay was performed as described in Figure 4. DMSO, vehicle control. Luminescence intensities represented as percentages.

Compound **1**, assayed in parallel, did not show anti-HIV activity in MT-4 cells at concentrations lower than its CC_{50} value, whereas a marked activity was measured in OM-10.1 cells, where however the stronger cytotoxicity led to a SI value of 60, lower than that of **37**.

Intriguingly, the antiviral activity observed in latently infected cells with compound **37** was higher than what observed in the kinase assay and in the LTR-luciferase assay, suggesting that an additive mechanism might contribute to the antiviral effect. Therefore, we investigated other kinases that are involved in the Tat-mediated transcription process and that share structural features with CDK9. We focused our attention on CDK2, which is emerging as a valid target[48] being not essential for mammalian development[49,50] but required for Tat-dependent transcription.[51,52] Specifically, CDK2 in complex with cyclin E phosphorylates the RNAPII CTD once recruited to the promoter by Tat, which is itself a target of CDK2-mediated phosphorylation. CDK2 also phosphorylates CDK9 on Ser90, as recently reported.[53] Indeed, when compound **37** was tested on CDK2, an inhibition comparable to that obtained on CDK9 was observed with and IC_{50} value of 3.39 μm.

An insight into the double activity of **37** can be achieved looking at the predicted binding mode into both enzymes along with the comparison to several published crystallographic structures and literature data showing the chemical features needed to obtain selectivity.[24,54–59] Compound **37**, in its docking-predicted pose, binds to the ATP pocket engaging in hydrogen-bond interactions with the backbone of CDK9 Cys106/CDK2 Leu83 and making contacts with several residues conserved among the two enzymes. Although the two binding sites share a high number of structural features, some peculiar differences have been shown to be exploitable to impart selectivity to ligands towards one of the two enzymes.[54,56,57,59] The region around CDK2 Lys88 and Lys89 (cyan sphere) is more closed in CDK2, since the two residues are bulkier than the corresponding CDK9 Ala111 and Gly112 (Figure 6). Indeed, rigid and bulky substituents in the zone highlighted by the cyan sphere would hamper ligand binding to CDK2 because of steric clash with the Lys residue, whereas flexible substituents capable of accepting a hydrogen bond from Lys89 would probably result in a more efficient binding to CDK2. The loop comprising CDK9 residues 25–32 (10–17 on CDK2) has been observed to rearrange, moving towards the ATP binding site upon binding of several diverse competitive inhibitors on CDK9 [24,54] and thus offering the possibility to take advantage of this structural difference to obtain CDK9 selectivity by using substituents capable of engaging interaction with the loop residues (green sphere, Figure 6). Another structural difference between the two enzymes was observed in the region marked by the pink sphere, where CDK9 Glu66 can move away from the ATP binding site, thus making the binding pocket next to Phe168 larger than the same pocket in CDK2.
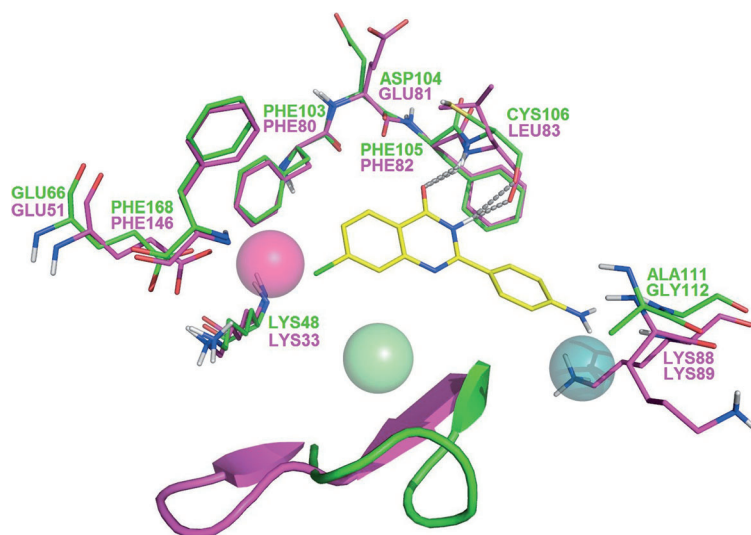

Figure 6. Predicted binding mode of **37** (yellow sticks) into the ATP pocket of CDK2 (PDB ID: 3TNW; magenta sticks and cartoon) and CDK9 (PDB ID: 3TNH; green sticks and cartoon). Hydrogen bonds are shown as dashed grey lines. The loops comprising CDK9 residues 25–32 (10–17 on CDK2) are represented as cartoon. This Figure was prepared using PyMOL.[80]

In its predicted bound conformation, **37** does not overlap but is next to the above described exploitable features that could be used to optimize activity toward CDK9 or CDK2 or design a single molecule endowed with both activities, thus making our low-weight compounds highly optimizable in both potency and selectivity.

Conclusions

Tat-mediated transactivation is an attractive target for anti-HIV-1 therapy because it controls a key step during reactivation from latency. The kinase subunit of the positive transcription elongation factor b (P-TEFb) complex that is recruited by Tat to the viral promoter is a potential target. In this work, we took advantage of the crystallographic data of cyclin-dependent kinase 9 (CDK9) in complex with **1** and used it for the design and synthesis of novel inhibitors. We have identified quinazolinone fragment **2** endowed with a residual anti-CDK9 activity at 500 μm that was improved by just adding a phenyl substituent at the C-2 position as in derivatives **3** and **4**. These compounds were then elaborated by a combination of different medicinal chemistry approaches, leading to analogues **16**, **23**, **24**, **26**, and **37**, which inhibited CDK9 with IC_{50} values in the micromolar range. With the exception of compound **16**, these 2-phenyl-quinazolinones were able to inhibit Tat-mediated transactivation in cell lines, with 7-chloro derivative **37** being the most potent. Notably, the inhibitory activity was specific to Tat-mediated transactivation. More interestingly, the inhibition of Tat-mediated transactivation translated into the ability to inhibit HIV-1 reactivation from latently infected cells, with compound **37** showing a potency that was superior to what could be predicted looking at its CDK9 activity, thus leading to the hypothesis of an additional target. Indeed, CDK2, which plays a sup-

portive role within the transcriptional machinery and shares structural features with CDK9, was also inhibited by compound **37** at comparable concentrations.

The appeal of the reported 2-phenylquinazolinones are strengthened by the lack of toxicity in several cell lines, which, coupled with the inability to influence the basal transcription, suggests a selective action towards the Tat-hijacked CDKs. In addition, as these compounds merely represent fragments,[60] there is plenty of room for further optimization, which will of course require an overall kinase inhibition profiling, once more potent compounds are obtained.

Experimental Section

Chemistry

All reactions were routinely checked by thin-layer chromatography (TLC) on silica gel 60 F_{254} (Merck) and visualized using UV light or iodine. Flash column chromatography separations were carried out on silica gel 60 (mesh 230–400, Merck). Melting points (mp) were determined in capillary tubes using an Electrothermal 9100 (Büchi, Essen, Germany) and are uncorrected. Elemental analyses were performed on a EA1108CHN elemental analyzer (Fisons, Ipswich, UK), and the data for C, H and N are within ±0.4% of the theoretical values. ^{1}H NMR and ^{13}C NMR spectra were recorded at 200 MHz (Bruker Avance DPX-200) and 400 MHz (Bruker Avance DRX-400) using residual solvents such as CHCl$_3$ ($\delta = 7.26$ ppm) or dimethyl sulfoxide (DMSO, $\delta = 2.48$ ppm) as internal standard. Chemical shifts (δ) are given in ppm, and the spectral data are consistent with the assigned structures. Reagents and solvents were purchased from common commercial suppliers and were used as such. After extraction, organic solutions were dried over anhydrous Na$_2$SO$_4$, filtered, and concentrated with a Büchi rotary evaporator at reduced pressure. Yields are of purified product and were not optimized. All starting materials were commercially available unless otherwise indicated.

Compound **2** was purchased from Sigma–Aldrich (code H57807), compound **3** was purchased from Enamine (code T6147622; NJ, USA) and **4** was purchased from Princeton Biomolecular Research (code OSSK540864; NJ, USA). Their identity was independently assessed by ^{1}H NMR (see Supporting Information).

2-(4-Propoxyphenyl)quinazolin-4(3H)-one (9): NH$_4$OAc (0.3 g, 4.12 mmol), 4-propoxybenzaldehyde (0.6 g, 4.12 mmol), I$_2$ (2.7 g, 10.97 mmol), and powdered KOH (0.2 g, 4.12 mmol) were added to a solution of isatoic anhydride (0.5 g, 3.4 mmol) in N,N-dimethylformamide (DMF; 10 mL), and the solution was stirred at 85 °C for 4 h. After cooling, the reaction mixture was poured into ice water and extracted with EtOAc. The organic layers were evaporated to dryness to give a residue that was purified by flash chromatography eluting with MeOH/CHCl$_3$ (5% v/v), and then crystallized from EtOH to give **9** as white crystals (0.57 g, 60%): mp: 212–215 °C; ^{1}H NMR (400 MHz, [D$_6$]DMSO): $\delta = 12.50$ (bs, 1H, CONH), 8.15–8.25 (m, 3H, H-5, H-3′, and H-5′), 7.80–7.85 (dt, J = 7.0 and 2.0 Hz, 1H, H-6), 7.35–7.45 (dt, J = 8.0 Hz and 1.0 Hz, 1H, H-7), 7.65 (d, J = 8.0 Hz, 1H, H-8), 7.00 (d, J = 8.0 Hz, 2H, H-2′ and H-6′), 4.00 (t, J = 7.0 Hz, 2H, OCH$_2$), 1.65–1.75 (m, 2H, OCH$_2$CH$_2$), 1.00 ppm (t, J = 7.0 Hz, 3H, CH$_2$CH$_3$); ^{13}C NMR (100 MHz, [D$_6$]DMSO): $\delta = 10.7$, 22.4, 69.6, 114.8, 121.1, 125.0, 126.2, 126.5, 127.7, 130.0, 134.9, 149.3, 152.3, 161.4, 162.7 ppm; Anal. calcd for C$_{17}$H$_{16}$N$_2$O$_2$: C 78.84, H 5.75, N 9.99, found: C 78.99, H 5.85, N 9.95.

2-(4-Ethoxyphenyl)quinazolin-4(3H)-one (10): The synthetic procedure for **9** was used, replacing 4-propoxybenzaldehyde with 4-ethoxybenzaldehyde, to give **10** as white crystals (0.50 g; 55%): mp: 254–255 °C; ^{1}H NMR (400 MHz, [D$_6$]DMSO): $\delta = 12.50$ (bs, 1H, CONH), 8.10–8.20 (m, 3H, H-5, H-3′, and H-5′), 7.60–7.80 (m, 2H, H-6 and H-8), 7.45 (dt, J = 7.0 and 1.0 Hz, 1H, H-7), 7.10 (d, J = 8.0 Hz, 2H, H-2′ and H-6′), 4.10 (q, J = 7.5 Hz, 2H, OCH$_2$), 1.40 ppm (t, J = 7.5 Hz, 3H, OCH$_2$CH$_3$); ^{13}C NMR (100 MHz, [D$_6$]DMSO): $\delta = 11.2$, 65.6, 115.0, 121.1, 125.3, 126.7, 126.9, 127.8, 130.1, 134.6, 149.8, 152.8, 161.5, 162.0 ppm; Anal. calcd for C$_{16}$H$_{14}$N$_2$O$_2$: C 72.16, H 5.30, N 10.52, found: C 72.00, H 5.20, N 10.60.

2-(4-Isopropoxyphenyl)quinazolin-4(3H)-one (11): The synthetic procedure for **9** was used, replacing 4-propoxybenzaldehyde with 4-isopropoxybenzaldehyde, to give **11** as white crystals (0.55 g; 58%): mp: 236–238 °C; ^{1}H NMR (400 MHz, [D$_6$]DMSO): $\delta = 12.50$ (bs, 1H, CONH), 8.10–8.20 (m, 3H, H-5, H-3′, and H-5′), 7.70–7.80 (m, 2H, H-6 and H-8), 7.45 (dt, J = 7.0 and 1.0 Hz, 1H, H-7), 7.10 (d, J = 8.0 Hz, 2H, H-2′ and H-6′), 4.55–4.65 (m, 1H, OCH), 1.20 ppm (d, J = 6.0 Hz, 6H, CH(CH$_3$)$_2$); ^{13}C NMR (100 MHz, [D$_6$]DMSO): $\delta = 22.0$, 66.8, 114.9, 121.3, 124.8, 125.2, 126.8, 126.9, 127.3, 129.9, 131.0, 134.6, 149.8, 152.1, 161.5, 162.0 ppm; Anal. calcd for C$_{17}$H$_{16}$N$_2$O$_2$: C 72.84, H 5.75, N 9.99, found: C 73.10, H 5.75 N 10.10.

4-(3-Methylbutoxy)benzaldehyde (42): 1-Iodo-3-methylbutane (0.81 mL, 6.15 mmol) was added to a suspension of 4-hydroxybenzaldehyde (0.50 g, 4.10 mmol) and K$_2$CO$_3$ (0.85 g, 6.15 mmol) in CH$_3$CN. The suspension was allowed to stir at reflux for 5 h. After cooling to RT, the suspension was filtered, and the solution was evaporated in vacuo to give **42** as a yellow oil (0.78 g; 99%): ^{1}H NMR (400 MHz, [D$_6$]DMSO): $\delta = 9.95$ (s, 1H, COH), 7.80–7.85 (m, 2H, H-3′, and H-5′), 7.10–7.15 (m, 2H, H-2′ and H-6′), 4.05 (t, J = 6.0 Hz, 2H, OCH$_2$), 1.50–1.80 (m, 3H, CHCH$_2$), 0.95 ppm (d, J = 7.0 Hz, 6H, CH(CH$_3$)$_2$).

2-[4-(3-Methylbutoxy)phenyl]quinazolin-4(3H)-one (12): The synthetic procedure for **9** was used, replacing 4-propoxybenzaldehyde with **42**, to give **12** as a white powder (0.49 g; 47%): mp: 181–184 °C; ^{1}H NMR (400 MHz, [D$_6$]DMSO): $\delta = 12.50$ (bs, 1H, CONH), 8.05–8.15 (m, 3H, H-5, H-3′, and H-5′), 7.60–7.80 (m, 2H, H-6 and H-8), 7.45 (dt, J = 7.0 and 1.0 Hz, 1H, H-7), 7.10 (d, J = 8.0 Hz, 2H, H-2′ and H-6′), 4.10 (t, J = 6.0 Hz, 2H, OCH$_2$), 1.60–1.80 (m, 3H, CH$_2$CH), 0.9 ppm (d, J = 6.0 Hz, 6H, CH(CH$_3$)$_2$); ^{13}C NMR (100 MHz, [D$_6$]DMSO): $\delta = 22.83$, 25.03, 37.76, 66.67, 114.83, 121.12, 125.06, 126.25, 126.48, 127.70, 129.87, 134.91, 149.39, 152.30, 161.75, 162.74 ppm; Anal. calcd for C$_{19}$H$_{20}$N$_2$O$_2$: C 74.00, H 6.54, N 9.08, found: C 74.25, H 6.54, N 9.20.

2-(4-Aminophenyl)quinazolin-4(3H)-one (16):[36] The synthetic procedure for **9** was used, replacing 4-propoxybenzaldehyde with 4-aminobenzaldehyde, to give **16** as a light-yellow powder (0.47 g; 58%): mp: 280–282 °C; ^{1}H NMR (400 MHz, [D$_6$]DMSO): $\delta = 12.10$ (bs, 1H, CONH), 8.05–8.15 (m, 1H, H-5), 7.90 (d, J = 8.0 Hz, 2H, H-2′ and H-6′), 7.75 (t, J = 7.0 Hz, 1H, H-7), 7.65 (d, J = 8.0 Hz, 1H, H-8), 7.40 (t, J = 7.0 Hz, 1H, H-6), 6.60 (d, J = 8.0 Hz, 2H, H-3′ and H-5′), 5.85 ppm (bs, 2H, NH$_2$); ^{13}C NMR (100 MHz, [D$_6$]DMSO): $\delta = 114.2$, 121.6, 125.7, 126.2, 126.4, 127.6, 130.1, 135.1, 149.6, 152.0, 156.4, 162.0 ppm; Anal. calcd for C$_{14}$H$_{11}$N$_3$O: C 70.87, H 4.67, N 17.71, found: C 71.00, H 4.80, N 17.67.

2-(1H-Imidazol-5-yl)quinazolin-4(3H)-one (17): The synthetic procedure for **9** was used, replacing 4-propoxybenzaldehyde with 1H-imidazole-5-carbaldehyde, to give **17** as a white powder (0.28 g; 40%): mp: 256–258 °C; ^{1}H NMR (400 MHz, [D$_6$]DMSO): $\delta = 12.00$ (bs, 1H, CONH), 10.10 (bs, 1H, NH), 8.20 (d, J = 8 Hz, 1H, H-5), 8.00 (s, 1H, H-5′), 7.85 (s, 1H, H-3′), 7.75–7.80 (m, 1H, H7), 7.65 (d, J = 8 Hz,

1H, H-8), 7.45 ppm (t, $J = 8.0$ Hz, 1H, H-6); ^{13}C NMR (100 MHz, [D$_6$]DMSO): $\delta = 105.9$, 123.2, 124.2, 126.3, 129.4, 131.9, 138.6, 142.9, 148.0, 163.1 ppm; Anal. calcd for C$_{11}$H$_8$N$_4$O: C 62.26, H 3.80, N 26.40, found: C 62.30, H 3.92, N 26.43.

2-(2-Chloro-3-hydroxy-4-methoxyphenyl)quinazolin-4(3H)-one (18): The synthetic procedure for **9** was used, replacing 4-propoxybenzaldehyde with 2-chloro-3-hydroxy-4-methoxybenzaldehyde, to give **18** as colorless crystals (0.60 g; 53%): mp: 276–279 °C; ^{1}H NMR (400 MHz, [D$_6$]DMSO): $\delta = 12.50$ (bs, 1H, CONH), 9.65 (bs, 1H, OH), 8.25 (dd, $J = 1.0$ and 8.0 Hz, 1H, H-5), 7.80 (dt, $J = 7.0$ and 2.0 Hz, 1H, H-6), 7.70 (d, $J = 8.0$ Hz, 1H, H-8), 7.55 (t, $J = 8.0$ Hz, 1H, H-7), 6.95–7.05 (m, 2H, H-5′ and H-6′), 3.90 ppm (s, 3H, OCH$_3$); ^{13}C NMR (100 MHz, [D$_6$]DMSO): $\delta = 56.6$, 112.7, 114.8, 121.5, 125.1, 126.2, 127.4, 127.9, 132.9, 135.0, 149.2, 151.3, 156.9, 161.7 ppm; Anal. calcd for C$_{15}$H$_{11}$ClN$_2$O$_3$: C 59.52, H 3.66, N 9.25, found: C 59.20, H 3.47, N 9.41.

2-(4-Pyridin-2-ylphenyl)quinazolin-4(3H)-one (19): The synthetic procedure for **9** was used, replacing 4-propoxybenzaldehyde with 4-pyridin-2-ylbenzaldehyde, to give **19** as a white powder (0.46 g; 46%): mp: 279–282 °C; ^{1}H NMR (400 MHz, [D$_6$]DMSO): $\delta = 12.5$ (bs, 1H, CONH), 8.70 (dd, $J = 8.0$ and 1.0 Hz, 1H, pyridine CH), 8.30 (d, $J = 8.0$ Hz, 2H, H-2′ and H-6′), 8.25 (d, $J = 8.0$ Hz, 2H, H-3′ and H-5′), 8.15–8.20 (m, 1H, pyridine CH), 8.10 (d, $J = 8$ Hz, 1H, H-5), 7.90–7.95 (m, 1H, pyridine CH), 7.85 (dt, $J = 7.0$ and 2.0 Hz, 1H, H-6), 7.75 (d, $J = 8.0$ Hz, 1H, H-8), 7.55 (dt, $J = 7.0$ and 1.0 Hz, 1H, H-7), 7.35–7.40 ppm (m, 1H, pyridine CH); ^{13}C NMR (100 MHz, [D$_6$]DMSO): $\delta = 121.2$, 121.4, 123.7, 126.3, 127.0, 127.1, 127.9, 128.6, 133.4, 135.0, 141.5, 149.0. 150.1, 152.3, 155.2, 161.8 ppm; Anal. calcd for C$_{19}$H$_{13}$N$_3$O: C 76.24, H 4.38, N 14.04, found: C 76.33, H 4.37, N 14.00.

2-(5-Bromo-2-methoxyphenyl)quinazolin-4(3H)-one (20):[37] The synthetic procedure for **9** was used, replacing 4-propoxybenzaldehyde with 5-bromo-2-methoxybenzaldehyde, to give **20** as a white powder (0.55 g; 49%): mp: 178–182 °C; ^{1}H NMR (400 MHz, [D$_6$]DMSO): $\delta = 12.20$ (bs, 1H, CONH), 8.10 (d, $J = 8.0$ Hz, 1H, H-5), 7.80–7.85 (m, 2H, H-7 and H-6′), 7.60–7.75 (m, 2H, H-8 and H-4′), 7.55 (t, $J = 7$ Hz, 1H, H-6), 7.20 (d, $J = 9.0$ Hz, 1H, H-3′), 3.80 ppm (s, 3H, OCH$_3$); ^{13}C NMR (100 MHz, [D$_6$]DMSO): $\delta = 56.6$, 112.7, 114.8, 121.5, 125.1, 126.2, 127.4, 127.9, 132.9, 135.0, 149.2, 151.3, 156.9, 161.7 ppm; Anal. calcd for C$_{15}$H$_{11}$BrN$_2$O$_2$: C 54.40, H 3.35, N 8.46, found: C 54.70, H 3.21, N 8.60.

2-(4-Piperidin-1-ylphenyl)quinazolin-4(3H)-one (21):[38] The synthetic procedure for **9** was used, replacing 4-propoxybenzaldehyde with 4-piperidin-1-ylbenzaldehyde, to give **21** as a grey powder (0.63 g; 61%): mp: 274–277 °C; ^{1}H NMR (400 MHz, [D$_6$]DMSO): $\delta = 12.20$ (bs, 1H, CONH), 8.10 (d, $J = 9.0$ Hz, 3H, H-5, H-3′, and H-5′), 7.80 (dt, $J = 7.0$ and 1.0 Hz, 1H, H-7), 7.65 (d, $J = 8.0$ Hz, 1H, H-8), 7.45 (t, $J = 7.0$ Hz, 1H, H-6), 7.00 (d, $J = 9.0$ Hz, 2H, H-6′ and H-2′), 3.30 ppm (s, 10H, piperidine CH$_2$); ^{13}C NMR (100 MHz, [D$_6$]DMSO): $\delta = 24.4$, 25.3, 48.5, 114.2, 120.8, 125.8, 126.0, 126.2, 127.5, 129.4, 134.9, 149.7, 152.5, 153.4, 162.8 ppm; Anal. calcd for C$_{19}$H$_{22}$N$_2$O$_2$: C 73.52, H 7.14, N 9.03, found: C 73.62, H 7.30, N 9.00.

2-(4-Hydroxy-1-naphthyl)quinazolin-4(3H)-one (22): The synthetic procedure for **9** was used, replacing 4-propoxybenzaldehyde with 4-hydroxy-1-naphthaldehyde, to give **22** as a light-pink powder (0.56 g; 57%): mp: 263–267 °C; ^{1}H NMR (400 MHz, [D$_6$]DMSO): $\delta = 12.45$ (bs, 1H, CONH), 10.75 (bs, 1H, OH), 8.20–8.30 (m, 2H, H-8′ and H-5′), 8.10–8.15 (m, 1H, H-5), 7.85 (dt, $J = 7.0$ and 1.0 Hz, 1H, H-7), 7.70 (d, $J = 8.0$ Hz, 1H, H-8), 7.65 (d, $J = 8.0$ Hz, 1H, H-3′), 7.50–7.55 (m, 3H, H-6, H-6′, and H-7′), 7.00 (d, $J = 8.0$ Hz, 1H, H-2′), 4.30 (bt, $J = 5.0$ Hz, 0.3H, CH$_2$OH), 3.40–3.50 (m, 6H, CH$_2$), 1.10 ppm (t,

$J = 7.0$, 0.9H, CH$_3$); ^{13}C NMR (100 MHz, [D$_6$]DMSO): $\delta = 18.9$, 56.4, 107.5, 121.3, 122.6, 122.7, 124.9, 125.4, 125.5, 126.2, 126.8, 127.6, 127.7, 129.7, 132.2, 134.8, 149.3, 154.3, 155.8, 162.5 ppm; Anal. calcd for C$_{18}$H$_{12}$N$_2$O$_2$·1/3 C$_2$H$_5$OH): C 71.84, H 5.43, N 8.38, found: C 72.00, H 5.55, N 8.25.

2-(1H-Indazol-5-yl)quinazolin-4(3H)-one (23): The synthetic procedure for **9** was used, replacing 4-propoxybenzaldehyde with 1H-indazole-5-carbaldehyde, to give **23** as a white powder (0.37 g; 42%): mp: 340–343 °C; ^{1}H NMR (400 MHz, [D$_6$]DMSO): $\delta = 13.35$ (bs, 1H, NH), 12.50 (bs, 1H, CONH), 8.70 (s, 1H, H-3′), 8.20–8.25 (m, 2H, H-2′, and H-7′), 8.15 (d, $J = 8.0$ Hz, 1H, H-5), 7.85 (t, $J = 7.0$ Hz, 1H, H-7), 7.75 (d, $J = 8.0$ Hz, 1H, H-8), 7.70 (d, $J = 9.0$ Hz, 1H, H-6′), 7.50 ppm (t, $J = 7$ Hz, 1H, H-6); ^{13}C NMR (100 MHz, [D$_6$]DMSO): $\delta = 108.1$, 116.3, 120.9, 121.8, 124.5, 125.2, 127.3, 134.2, 141.8, 150.0, 157.8, 161.5 ppm; Anal. calcd for C$_{15}$H$_{10}$N$_4$O: C 68.69, H 3.84, N 21.36, found: C 68.88, H 4.95, 21.20.

2-{4-[(2-Hydroxyethyl)(methyl)amino]phenyl}quinazolin-4(3H)-one (24): NH$_4$OAc (0.46 g, 6.00 mmol), 4-[(2-hydroxyethyl)-(methyl)amino]benzaldehyde (0.89 g, 5.0 mmol), and Yb(OTf)$_3$ (0.03 g, 0.05 mmol) were added to a solution of isatoic anhydride (0.89 g, 5.50 mmol) in DMSO (5 mL), and the mixture was maintained at 90 °C for 15 h. After cooling, the reaction mixture was poured into ice water, obtaining a precipitate, which was filtered and crystallized from EtOH, to give **24** as a light-yellow powder (0.09 g, 40%): mp: 220–223 °C; ^{1}H NMR (400 MHz, [D$_6$]DMSO): $\delta = 12.00$ (bs, 1H, CONH), 7.95–8.05 (m, 3H, H-5, H-3′, and H-5′), 7.75 (t, $J = 7.0$ Hz, 1H, H-7), 7.65 (d, $J = 8.0$ Hz, 1H, H-8), 7.45 (t, $J = 7.0$ Hz, 1H, H-6), 6.75 (d, $J = 8.0$ Hz, 2H, H-2′ and H-6′), 4.70–4.80 (m, 1H, OH), 3.50–3.60 (m, 4H, NCH$_2$CH$_2$O), 3.00 ppm (s, 3H, NCH$_3$); ^{13}C NMR (100 MHz, [D$_6$]DMSO): $\delta = 39.1$, 54.2, 58.2, 111.3, 118.7, 120.8, 125.7, 126.2, 127.4, 129.3, 134.8, 149.8, 151.8, 152.6, 162.8 ppm; Anal. calcd for C$_{17}$H$_{17}$N$_3$O$_2$: C 69.14, H 5.80, N 14.23, found: C 69.00, H 5.98, N 14.21.

2-Isoquinolin-5-ylquinazolin-4(3H)-one (25) and 2-isoquinolin-5-yl-2,3-dihydroquinazolin-4(1H)-one (41): The synthetic procedure for **24** was used, replacing 4-[(2-hydroxyethyl)-(methyl)amino]benzaldehyde with isoquinoline-5-carbaldehyde, to give **25** and **41**, respectively, after purification by flash chromatography eluting with EtOH/CHCl$_3$ (5% v/v).

25 (0.38 g; 41%): white powder; mp: 318–320 °C; ^{1}H NMR (400 MHz, [D$_6$]DMSO): $\delta = 12.75$ (bs, 1H, CONH), 9.45 (s, 1H, H-5′), 8.60 (d, $J = 6.0$ Hz, 1H, H-3′), 8.30 (d, $J = 8.0$ Hz, 1H, H-5), 8.10–8.25 (m, 3H, H-8′, H-6′, and H-2′), 7.80–7.90 (m, 2H, H-7, and H-7′), 7.75 (d, $J = 8.0$ Hz, 1H, H-8), 7.50 ppm (t, $J = 7.0$ Hz, 1H, H-6); ^{13}C NMR (100 MHz, [D$_6$]DMSO): $\delta = 118.5$, 121.7, 126.3, 127.1, 127.4, 127.9, 128.6, 130.7, 130.8, 132.5, 133.2, 135.0, 144.3, 149.0, 152.8. 153.3, 162.4 ppm; Anal. calcd for C$_{17}$H$_{11}$N$_3$O: C 74.71, H 4.06, N 15.38, found: C 74.78, H 4.19, N 15.25.

41 (0.33 g; 36%): white crystals; mp: 227–230 °C; ^{1}H NMR (400 MHz, [D$_6$]DMSO): $\delta = 9.40$ (s, 1H, H-5′), 8.55 (d, $J = 6.0$ Hz, 1H, H-3′), 8.35 (d, $J = 6.0$ Hz, 1H, H-2′), 8.30 (bs, 1H, CONH), 8.20 (d, $J = 8.0$ Hz, 1H, H-5), 7.90 (d, $J = 8.0$ Hz, 1H, H-8), 7.60–7.70 (m, 2H, H-7 and H-7′), 7.25 (t, $J = 7.0$ Hz, 1H, H-6), 7.10 (bs, 1H, CNH), 6.65–6.70 (m, 2H, H-8′ and H-6′), 6.50 (bs, 1H, CH); ^{13}C NMR (100 MHz, [D$_6$]DMSO): $\delta = 68.2$, 112.5, 114.6, 115.8, 118.3, 123.2, 126.2, 127.2, 128.0, 128.7, 129.2, 129.6, 133.5, 145.7, 146.6, 155.2, 162.4 ppm; Anal. calcd for C$_{17}$H$_{13}$N$_3$O: C 74.17, H 4.76, N 15.26, found: C 74.00, H 4.95, N 15.18.

2-(2,3,4-Trihydroxyphenyl)quinazolin-4(3H)-one (26): p-Toluenesulfonic acid (pTsOH; 0.03 g, 0.22 mmol) was added to a suspension

of 2-aminobenzamide (0.3 g, 2.20 mmol) and 2,3,4-trihydroxyben-zaldehyde (0.40 mg, 2.64 mmol) in MeOH (6.5 mL), and the mixture was heated at reflux for 5 h. After cooling, the obtained precipitate was filtered and washed several times with cold MeOH and crystallized from a mixture of EtOH/DMF to give **26** as a white powder (0.14 g, 43 %): mp: 332–335 °C; ^{1}H NMR (400 MHz, [D$_6$]DMSO): $\delta =$ 12.50 (bs, 1H, CONH) 8.15, 9.75, and 14.50 (bs, each 1H, OH), 8.15 (d, $J = 8.0$ Hz, 1H, H-5), 7.90 (t, $J = 8.0$ Hz, 1H, H-7), 7.60–7.70 (m, 2H, H-8 and H-2′), 7.50 (t, $J = 8.0$ Hz, 1H, H-6), 6.40 ppm (d, $J = 9.0$ Hz, 1H, H-3′); ^{13}C NMR (100 MHz, [D$_6$]DMSO): $\delta = 105.6$, 110.0, 117.1, 120.6, 121.6, 122.7, 123.0, 133.5, 135.4, 146.4, 150.5, 151.4, 154.9, 161.8 ppm; Anal. calcd for C$_{14}$H$_{10}$N$_2$O$_4$: C 62.22, H 3.73, N 10.37, found: C 62.32, H 3.99, N 10.37.

2-[4-(Diethylamino)phenyl]quinazolin-4(3H)-one (33):[39] The synthetic procedure for **9** was used, replacing 4-propoxybenzaldehyde with 4-(diethylamino)benzaldehyde, to give **33** as a white powder (0.53 g, 53 %): mp: 207–209 °C; ^{1}H NMR (400 MHz [D$_6$]DMSO): $\delta =$ 12.15 (s, 1H, CONH), 8.10 (m, 3H, H-5, H-2′, and H-6′), 7.80 (t, $J =$ 8.0 Hz, 1H, H-7), 7.70 (d, $J = 8.0$ Hz, 1H, H-8), 7.40 (t, $J = 7.0$ Hz, 1H, H-6), 6.80 (d, $J = 9.0$ Hz, 2H, H-3′ and H-5′), 3.45–3.50 (q, $J = 7.0$ Hz, 4H, NCH$_2$), 3.85 ppm (t, $J = 7.0$ Hz, 6H, CH$_3$); ^{13}C NMR (100 MHz, [D$_6$]DMSO): $\delta = 12.85$, 42.1, 111.0, 118.2, 120.7, 125.7, 126.2, 127.3, 129.6, 134.9, 149.8, 150.1, 152.7, 162.9 ppm; Anal. calcd for C$_{18}$H$_{19}$N$_3$O: C 73.69, H 6.53, N 14.32, found: C 73.69, H 6.55, N 14.26.

7-Chloro-2-(4-methoxyphenyl)quinazolin-4(3H)-one (35):[40] The synthetic procedure for **9** was used, replacing isatoic anhydride and 4-propoxybenzaldehyde with 7-chloro-isatoic anhydride and 4-methoxybenzaldehyde, respectively, to give **35** as a light-green powder (0.52 g, 54 %): mp: 277–280 °C; ^{1}H NMR (400 MHz [D$_6$]DMSO): $\delta = 3.85$ (s, 3H, OCH$_3$), 7.10 (d, $J = 8.0$ Hz, 2H, H-3′ and H-5′), 7.50 (dd, $J = 2.0$ and 9.0 Hz, 1H, H-6), 7.75 (d, $J = 2.0$ Hz, 1H, H-8), 8.10 (d, $J = 9.0$ Hz, 1H, H-5), 8.20 (d, $J = 8.0$ Hz, 2H, H-2′ and H-6′), 12.50 ppm (s, 1H, CONH); ^{13}C NMR (100 MHz, [D$_6$]DMSO): $\delta =$ 55.9, 114.5, 119.8, 124.7, 126.7, 126.8, 128.3, 130.1, 139.6, 150.4, 153.7, 162.1, 162.5 ppm; Anal. calcd for C$_{15}$H$_{11}$ClN$_2$O$_2$: C 62.84, H 3.87, N 9.77, found: C 62.48, H 4.05, N 9.59.

7-Chloro-2-{4-[(2-hydroxyethyl)-(methyl)amino]phenyl}quinazolin-4(3H)-one (36): The synthetic procedure for **9** was used, replacing isatoic anhydride and 4-propoxybenzaldehyde with 7-chloro-isatoic anhydride and 4-[(2-hydroxyethyl)(methyl)amino]benzaldehyde, respectively, to give **36** as white crystals (0.51 g; 46 %): mp: 250–251 °C; ^{1}H NMR (400 MHz [D$_6$]DMSO): $\delta = 12.50$ (bs, 1H, CONH), 8.05–8.15 (m, 3H, H-5, H-2′, and H-6′), 7.65 (d, $J = 2.0$ Hz,1H, H-8), 7.45 (dd, $J = 2.0$ and 9.0 Hz, 1H, H-6), 6.75 (d, $J = 9.0$ Hz, 2H, H-3′ and H-5′), 4.50 (bs, 1H, OH), 3.50 and 3.55 (t, $J = 6.0$ Hz, each 2H, NCH$_2$ and CH$_2$OH), 3.00 ppm (s, 3H, NCH$_3$); ^{13}C NMR (100 MHz, [D$_6$]DMSO): $\delta = 39.1$, 54.2, 58.5, 111.3, 118.1, 118.5, 125.9, 126.2, 128.3, 129.7, 139.4, 150.8, 152.1, 154.1, 162.3 ppm; Anal. calcd for C$_{17}$H$_{16}$ClN$_3$O$_2$: C 61.91, H 4.89, N 12.74, found: C 61.99, H 4.98, N 12.49.

2-{4-[(2-Hydroxyethyl)(methyl)amino]phenyl}-2,3-dihydroquinazolin-4(1H)-one (40): The synthetic procedure for **9** was used, replacing 4-propoxybenzaldehyde with 4-[(2-hydroxyethyl)-(methyl)amino]benzaldehyde, to give **40** as a white powder (0.43 g, 43 %): mp: 177–180 °C; ^{1}H NMR (400 MHz [D$_6$]DMSO): $\delta =$ 8.00 (bs, 1H, CONH), 7.65 (d, $J = 8.0$ Hz, 1H, H-5), 7.20–7.30 (m, 3H, H-7, H-3′, and H-5′), 6.90 (bs, 1H, NH), 6.60–6.70 (m, 4H, H-6, H-8, H-2′ and H-6′), 5.60 (bs, 1H, CH), 4.60 (bt, $J = 5.0$ Hz, 1H, OH), 3.45–3.55 (m, 2H, CH$_2$O), 3.30 (t, $J = 5.0$ Hz, 2H, NCH$_2$), 2.90 ppm (s, 3H, NCH$_3$); ^{13}C NMR (100 MHz, [D$_6$]DMSO): $\delta = 39.1$, 54.5, 58.3, 67.1,

111.6, 114.8, 115.4, 117.3, 127.7, 128.8, 133.5, 148.6, 149.8, 164.2 ppm; Anal. calcd for C$_{17}$H$_{19}$N$_3$O$_2$: C 68.67, H 6.44, N 14.13, found: C 68.70, H 6.10, N 14.21.

4-Chloro-2-[(4-nitrobenzoyl)amino]benzamide (44): 4-Nitrobenzoyl chloride (1.2 g, 6.44 mmol) was added to a mixture of 2-amino-4-chlorobenzamide (1.1 g, 6.44 mmol) and Et$_3$N (0.9 mL, 6.44 mmol) in tetrahydrofuran (THF; 9 mL). After stirring 6 h at RT, the reaction mixture was poured into ice water, obtaining a precipitate, which was filtered to give **44** (1.9 g, 71 %): mp: 350–351 °C; ^{1}H NMR (400 MHz [D$_6$]DMSO): $\delta = 13.40$ (bs, 1H, NH), 8.80 (d, $J = 2.0$ Hz, 1H, H-3), 8.60 (bs, 1H, NH$_2$), 8.45 (d, $J = 9.0$ Hz, 2H, H-3′ and H-5′), 8.00 (d, $J = 9.0$ Hz, 2H, H-2′ and H-6′), 7.95–8.05 (m, 2H, H-6 and 1H NH$_2$), 7.35 ppm (dd, $J = 2.0$ and 9.0 Hz, 1H, H-5).

7-Chloro-2-(4-nitrophenyl)quinazolin-4(3H)-one (38):[47] Potassium *tert*-butoxide (0.4 g, 3.55 mmol) was added portion wise to a suspension of **44** (0.2 g, 0.71 mmol) in *tert*-butanol (15 mL). After stirring 24 h at RT, the reaction mixture was evaporated to dryness to give a residue, which was treated with 2 N HCl. The obtained solid was filtered and crystallized from EtOH to give **38**[47] (0.15 g, 70 %): mp: 358–359 °C; ^{1}H NMR (400 MHz [D$_6$]DMSO): $\delta = 13.40$ (bs, 1H, CONH), 8.35–8.40 (m, 4H, H-2′, H-3′, H-5′, and H-6′), 8.20 (d, $J =$ 9.0 Hz, 1H, H-5), 7.90 (d, $J = 2.0$ Hz, 1H, H-8), 7.60 ppm (dd, $J = 2.0$ and 9.0 Hz, 1H, H-6); ^{13}C NMR (100 MHz, [D$_6$]DMSO): $\delta = 119.9$, 122.9124.2, 124.3, 127.6, 129.0, 135.6, 140.1, 146.7, 148.9, 156.7, 162.2 ppm; Anal. calcd for C$_{14}$H$_8$ClN$_3$O$_3$: C 55.74, H 2.67, N 13.96, found: C 56.04, H 2.81, N 13.85.

2-(4-Aminophenyl)-7-chloroquinazolin-4(3H)-one (37): A solution of **38**[47] (0.1 g, 0.3 mmol) in DMF (10 mL), was hydrogenated over a catalytic amount of Raney nickel at RT and atmospheric pressure for 2 h. The mixture was then filtered over Celite, and the filtrate was evaporated to dryness to afford a residue, which was crystallized from EtOH to give **37** (0.05 g, 60 %): mp: 350–351 °C; ^{1}H NMR (400 MHz [D$_6$]DMSO): $\delta = 12.20$ (bs, 1H, CONH), 8.10 (d, $J = 9.0$ Hz, 1H, H-5), 7.95 (d, $J = 8.0$ Hz, 2H, H-2′ and H-6′), 7.70 (d, $J = 2.0$ Hz, 1H, H-8), 7.40 (dd, $J = 2.0$ and 9.0 Hz, 1H, H-6), 6.60 (d, $J = 8.0$ Hz, 2H, H-3′ and H-5′), 6.00 ppm (bs, 2H, NH$_2$); ^{13}C NMR (100 MHz, [D$_6$]DMSO): $\delta = 113.5$, 118.6, 125.8, 126.3, 128.3, 129.7, 139.3, 151.0, 152.8, 154.2 162.3 ppm; Anal. calcd for C$_{14}$H$_{10}$ClN$_3$O: C 61.89, H 3.71, N 15.47, found: C 61.96, H 3.71, N 15.47.

Computational methods

Docking target preparation: The crystal structure of CDK9 in complex with cyclin T1 (CycT1) and flavopiridol was retrieved from the RCSB Protein Data Bank (PDB ID: 3BLR)[24] and used as target for our modeling studies. First, Schrödinger's Protein Preparation Wizard[61–63] was used to obtain satisfactory starting structures for docking studies. This facility is designed to ensure chemical correctness and to optimize a protein structure for further analysis. In particular, all water molecules were deleted, hydrogen atoms were added, bond orders and charges were then assigned, the orientation of hydroxy groups on Ser, Thr and Tyr, the side chains of Asn and Gln residues, and the protonation state of His residues were optimized. Moreover, the process relieves steric clashes by performing a series of restrained, partial minimizations on the co-crystallized structure, each of which employs a limited number of minimization steps. It was not intended to minimize the system completely. In our study, the minimization (OPLS 2005 force field)[64] was stopped when the root-mean square deviation (RMSD) values of the non-hydrogen atoms reached 0.30 Å, the specified limit by default. An enclosing box was used as docking space, centered on the active site using the corresponding ligand crystallographic po-

sition; the ligand diameter midpoint box was set to the default value (10 Å). No van der Waals (VdW) radii scaling was used. The same target preparation protocol was applied to crystal structures 3TNH and 3TNW.[57]

Docking of fragments: The Schrödinger fragment library was docked using Glide[65] in a stepwise manner. In particular, the library was first docked using Glide SP, using 0.80 to scale the VdW radii of the nonpolar ligand atoms with a charge cutoff of 0.15. Poses were discarded as duplicates if both RMSD values in the ligand-all atom was less than 1.5 Å and maximum atomic displacement was less than 2.3 Å. At most, two poses per ligand were retained. The obtained docking poses were then refined, rescored and minimized using Glide XP.

Ligand preparation: The structures of the molecules to screen were processed using the Schrödinger LigPrep utility.[66] This generates a number of low-energy 3D structures from each input molecule, with various ionization states, tautomers, stereochemistries, and ring conformations. For our study, a range of pH 6–8 was set, specified chiralities were retained, desalt was applied, tautomeric forms were obtained, and only one low-energy ring conformation per ligand was generated.

Virtual screening procedure: The compounds were screened using the virtual screening workflow of the Schrödinger Suite.[64] The databases were first docked with Glide HTVS and the 5% of the top-scoring molecules was submitted to Glide SP, keeping the 10% of the top-ranked molecules for the final docking and scoring by mean of Glide XP. All parameters of the three docking steps were kept as default.

Docking of 37 into 3TNW and 3TNH: Compound **37** was docked into both structures (PDBID: 3TNW and 3TNH) using Glide[65] in a stepwise manner. In particular, the compound was first docked using Glide SP, using 0.80 to scale the VdW radii of the nonpolar ligand atoms with a charge cutoff of 0.15. Poses were discarded as duplicates if both RMSD values in the ligand-all atom was less than 1.5 Å and the maximum atomic displacement was less than 2.3 Å. At most, three poses per ligand were retained. The obtained docking poses were then refined and rescored using Glide XP, retaining only the best scoring for each target. The resulting complexes were finally minimized through 500 steps of conjugate gradient minimization, using MM/GBSA[67] as solvation treatment and the optimized potentials for liquid simulations (OPLS) force field.[64]

MC/FEP calculations: Starting from the PDBID 3BLR, a reduced model of the protein was prepared using the residues comprised in a 15 Å distance from the ligand. The reduced protein model in complex with **2** was relaxed by 100 steps of conjugate gradient minimization. Monte Carlo (MC)/free energy perturbation (FEP) calculations were performed by means of MCPRO[68] following a standard 11 windows simple overlap sampling[69] protocol. TIP4P water model,[70] OPLS force-field[64] and CM^1A[71] ligand charges were employed. During the MC simulations, all degrees of freedom were sampled for the ligand; side chains of residues comprised in a distance of 10 Å from the ligand were sampled as well, whereas the protein backbone was kept fixed. For the two *ortho* and *meta* positions, the most energetically favorable substitution was selected, and an entropic penalty (0.6 kcal mol^{-1}) was applied for the loss of a rotameric state upon ligand binding.

Biology

CDK9 kinase assay: The cyclin-dependent kinase 9 (CDK9) activity was measured in vitro on a recombinant GST-CTD substrate as described previously.[72,73] Briefly, 293T cells were transfected with an expression plasmid for flag-tagged CDK9. The cells were collected 36 h post-transfection in NHEN buffer (20 mM HEPES pH 7.5, 300 mM NaCl, 0.5% NP-40, 20% glycerol, 1 mM EDTA, protease inhibitors) and sonicated. The lysate was clarified by centrifugation and incubated with anti-flag beads (M2; Sigma). The beads were then washed several times with NHEN buffer and kept for storage at $-20\,°C$ until use. The recombinant GST-CTD fusion protein was produced and purified from *E. coli* BL21.[74] Glutathione agarose beads were then washed extensively and kept frozen at $-20\,°C$ until use. For the kinase assay, the beads with GST-CTD and CDK9 were combined at 5:1 ratio and washed (3×) with fresh kinase buffer (50 mM Tris-HCl pH 7.4, 5 mM MgCl$_2$, 5 mM MnCl$_2$, 20 mM NaF, protease inhibitors; Roche). The beads were then supplemented with dithiothreitol (DTT; 2.5 mM), ATP (10 μM), [γ^{32}P]ATP (3 μCi) and inhibitor (1 μL) diluted in DMSO (vehicle). This reaction mixture was then incubated at 30°C for 30 min. The reaction was stopped by adding SDS sample buffer [100 mM Tris·HCl (pH 6.8), 4% sodium dodecyl sulfate (SDS), 0.2% bromophenol blue, 20% glycerol, 200 mM DTT] and boiling at 95°C, and samples were loaded into an 8% SDS-PAGE gel. After the run, the gels were stained with Coomassie blue, dried on 3M paper, and radioactivity was detected on a phosphor imaging system (Cyclone, Canberra Packard) and analyzed with OptiQuant (Packard).

CDK2 kinase assay: The biochemical activity of compounds was determined by incubation with cyclin-dependent kinase 2 (CDK2)/cyclin A and substrates, followed by quantification of the adenosine diphosphate (ADP) product by using the ADPGlo assay format (Promega). The recombinant GST-CDK2/cyclin A fusion protein was produced and purified as described previously;[75] Histone H1 and adenosine triphosphate (ATP) were commercially available (Sigma). Enzyme, Histone H1 and ATP, tested at 5 nM, 5 μM and 1 μM, respectively, were diluted in kinase buffer (50 mM Tris/HCl pH 7.5, 10 mM MgCl$_2$, 3 μM Na$_3$VO$_4$, 1 mM DTT, 0.2 mg mL^{-1} BSA). The compounds were threefold serially diluted in 100% DMSO followed by an intermediate dilution step in assay buffer in order to have a concentration curve from 139 μM to 0.007 μM in 1% DMSO. Kinase reactions were performed in a 96-well plate at RT for 30 min; flavopiridol and staurosporine were used as internal standards while positive controls (100% of inhibition, BOTTOM) in association with negative controls (no inhibition, TOP) were used to normalize data results. At the end of the incubation time, 25 μL of the kinase reaction was transferred in 96-well Optiplate (Greiner) in order stop the reaction and quantify the ADP generated by the ADPGlo assay. The luminescence signals were measured using ViewLux Reader (PerkinElmer, Boston, MA, USA). The raw data were analyzed using GraphPad Prism (version 5.2) by a four-parameter logistic equation, which provides sigmoidal fittings of the ten-dilution curves for IC$_{50}$ determination: $Y = BOTTOM + (TOP - BOTTOM)/(1 + 10((\log IC_{50} - X)*SLOPE))$, where X is the logarithm of the inhibitor concentration, Y is the response, SLOPE (Hill slope) is related to the stoichiometry of inhibitor enzyme interaction, TOP is the signal generated by the reaction without inhibitor and BOTTOM is the signal completely inhibited.

Cytotoxicity tests: Cytotoxicity in HeLa cells was assayed with Alamar blue (Invitrogen) as described in the product's specifications. Briefly, cells were seeded in a 96-well plate and incubated with the compounds at the indicated concentrations for 24 h before addition of the dye. After 24 h, the fluorescent signal was detected using a fluorimeter (Wallac plate reader, PerkinElmer).

Transactivation assay: The assay was performed as previously described.[73]

Anti-HIV-1 and cytotoxic assays in acutely infected MT-4 cells: Evaluation of the antiviral activity of the compounds against HIV-1 strain III_B in MT-4 cells was performed using the MTT assay as previously described.[76,77] Briefly, stock solutions (10× final concentration) of test compounds were added in 25 µL volumes to two series of triplicate wells so as to allow simultaneous evaluation of their effects on mock-and HIV-1-infected cells at the beginning of each experiment. Serial fivefold dilutions of test compounds were made directly in flat-bottomed 96-well microtiter trays using a Biomek® 3000 workstation (Beckman Coulter). Untreated control HIV-1- and mock-infected cell samples were included for each sample. HIV-1(III_B)[78] stock (50 µL) at 100–300 50 % cell culture infectious dose ($CCID_{50}$) or culture medium was added to either the infected or mock-infected wells of the microtiter tray. Mock-infected cells were used to evaluate the effect of test compound on uninfected cells in order to assess the cytotoxicity of the test compound. Exponentially growing MT-4 cells[79] were centrifuged for 5 min at 1000 rpm (220 g), and the supernatant was discarded. The MT-4 cells were resuspended at 6×10^5 cells mL^{-1}, and 50 µL volumes were transferred to the microtiter tray wells. Five days after infection, the viability of mock-and HIV-1-infected cells was examined spectrophotometrically using the MTT assay as described previously.[76] All data were calculated using the median optical density (OD) value of three wells. The CC_{50} was defined as the concentration of the test compound that reduced the absorbance (OD_{540}) of the mock-infected control sample by 50 %. The concentration achieving 50 % protection from the cytopathic effect of the virus in infected cells was defined as the EC_{50}.

Anti-HIV-1 and cytotoxic assays in latently infected OM-10.1 cells: The activity values of the compounds against latent HIV-1 infection were based on the inhibition of p24 antigen production in OM-10.1 cells after stimulation with phorbol 12-myristate 13-acetate (PMA; Sigma–Aldrich). Briefly, OM-10.1 cells (5×10^5 cells mL^{-1}) were incubated in the presence or absence of the compounds for 2 h in 48-well plates. After this short incubation period, the cells were stimulated with PMA (0.02 µM) followed by transfer of 2× 200 µL into a 96-well plate for toxicity evaluation. After a 2 day incubation at 37 °C, the cell-culture supernatants were collected from the 48-well plates and examined for their p24 antigen levels with the HIV-1 p24 ELISA kit (PerkinElmer). Cytotoxicity of the compounds for latently HIV-1-infected OM-10.1 cell line in the 96-well plates were based on the MTT cell viability staining as described previously.[76]

Supporting Information

Dose–response curve and histogram of virtual hit **2** (figure S1), CDK9 kinase assay for flavopiridol (**1**) (figure S2), dose–response curve of virtual hit **3** (figure S3), dose–response curve of virtual hit **4** (figure S4), cytotoxicity assay for compound **37** and **1** (figure S5), docking ranking, scores and anti-CDK9 activity of 14 selected virtual screening hits (table S1), FEP calculation results (table S2), docking ranking and scores of the molecules selected from the combinatorial library (table S3), elemental analysis data for resynthesized compounds **3** and **4**, (table S4), and ^{1}H NMR data for commercial compounds **2**, **3** and **4**.

Abbreviations

bs, broad singlet; cART, combination antiretroviral therapy; $CCID_{50}$, culture infectious dose; CDK2, cyclin dependent kinase 2; CDK9, cyclin dependent kinase 9; CTD, carboxy terminal domain; CycT1, cyclin T1; FEP, free energy perturbation;

HTVS, high-throughput virtual screening; LTR, long terminal repeat; OPLS, optimized potentials for liquid simulations; PMA, phorbol myristate acetate; P-TEFb, positive transcription elongation factor b; RNAPII, RNA polymerase II; SP, standard precision; TAR, Tat responsive element; XP, extra precision.

Acknowledgements

[1] L. Colin, C. Van Lint, *Retrovirology* **2009**, *6*, 111.
[2] A. Marcello, *Retrovirology* **2006**, *3*, 7.
[3] L. Shen, R. F. Siliciano, *J. Allergy Clin. Immunol.* **2008**, *122*, 22 – 28.
[4] J. Karn, *Curr. Opin. HIV AIDS* **2011**, *6*, 4 – 11.
[5] K. Chiba, J. Yamamoto, Y. Yamaguchi, H. Handa, *Exp. Cell Res.* **2010**, *316*, 2723 – 2730.
[6] H. S. Mancebo, G. Lee, J. Flygare, J. Tomassini, P. Luu, Y. Zhu, J. Peng, C. Blau, D. Hazuda, D. Price, O. Flores, *Genes Dev.* **1997**, *11*, 2633 – 2644.
[7] S. Massari, S. Sabatini, O. Tabarrini, *Curr. Pharm. Des.* **2013**, *19*, 1860 – 1879.
[8] W. Coley, K. Kehn-Hall, R. Van Duyne, F. Kashanchi, *Expert Opin. Biol. Ther.* **2009**, *9*, 1369 – 1382.
[9] O. Flores, G. Lee, J. Kessler, M. Miller, W. Schlief, J. Tomassini, D. Hazuda, *Proc. Natl. Acad. Sci. USA* **1999**, *96*, 7208 – 7213.
[10] L. M. Schang, *J. Antimicrob. Chemother.* **2002**, *50*, 779 – 792.
[11] Y. L. Chiu, H. Cao, J. M. Jacque, M. Stevenson, T. M. Rana, *J. Virol.* **2004**, *78*, 2517 – 2529.
[12] S. Wang, P. M. Fischer, *Trends Pharmacol. Sci.* **2008**, *29*, 302 – 313.
[13] Z. Yang, Q. Zhu, K. Luo, Q. Zhou, *Nature* **2001**, *414*, 317 – 322.
[14] L. Y. Liou, C. H. Herrmann, A. P. Rice, *J. Virol.* **2004**, *78*, 8114 – 8119.
[15] J. H. Yik, R. Chen, A. C. Pezda, C. S. Samford, Q. Zhou, *Mol. Cell. Biol.* **2004**, *24*, 5094 – 5105.
[16] A. Pumfery, C. de La Fuente, R. Berro, S. Nekhai, F. Kashanchi, S. H. Chao, *Curr. Pharm. Des.* **2006**, *12*, 1949 – 1961.
[17] S. Biglione, S. A. Byers, J. P. Price, V. T. Nguyen, O. Bensaude, D. H. Price, W. Maury, *Retrovirology* **2007**, *4*, 47.
[18] A. Ali, A. Ghosh, R. S. Nathans, N. Sharova, S. O'Brien, H. Cao, M. Stevenson, T. M. Rana, *ChemBioChem* **2009**, *10*, 2072 – 2080.
[19] G. Németh, Z. Varga, Z. Greff, G. Bencze, A. Sipos, C. Szántai-Kis, F. Baska, A. Gyuris, K. Kelemenics, Z. Szathmáry, J. Minárovits, G. Kéri, L. Orfi, *Curr. Med. Chem.* **2011**, *18*, 342 – 358.
[20] V. Krystof, S. Baumli, R. Fürst, *Curr. Pharm. Des.* **2012**, *18*, 2883 – 2890.
[21] A. Narayanan, G. Sampey, R. Van Duyne, I. Guendel, K. Kehn-Hall, J. Roman, R. Currer, H. Galons, N. Oumata, B. Joseph, L. Meijer, M. Caputi, S. Nekhai, F. Kashanchi, *Virology* **2012**, *432*, 219 – 231.
[22] O. Tabarrini, S. Massari, V. Cecchetti, *Future Med. Chem.* **2010**, *2*, 1161 – 1180.
[23] O. Tabarrini, S. Massari, L. Sancineto, D. Daelemans, S. Sabatini, G. Manfroni, V. Cecchetti, C. Pannecouque, *ChemMedChem* **2011**, *6*, 1249 – 1257.
[24] S. Baumli, G. Lolli, E. D. Lowe, S. Troiani, L. Rusconi, A. N. Bullock, J. E. Debreczeni, S. Knapp, L. N. Johnson, *EMBO J.* **2008**, *27*, 1907 – 1918.
[25] M. Congreve, R. Carr, C. Murray, H. Jhoti, *Drug Discovery Today* **2003**, *8*, 876 – 877.
[26] eMolecules. http://www.emolecules.com (accessed February 2010).

[27] Asinex. http://www.asinex.com/ (accessed February 2010).

[28] R. W. Zwanzig, *J. Chem. Phys.* **1954**, *22*, 1420–1427.

[29] CombiGlide, version 2.7, Schrödinger, LLC, New York, NY, **2011**.

[30] P. S. Reddy, P. P. Reddy, T. Vasantha, *Heterocycles* **2003**, *60*, 183–226.

[31] M. Baghbanzadeh, M. Dabiri, P. Salehi, *Heterocycles* **2008**, *75*, 2809–2815.

[32] L. Gao, H. Ji, L. Rong, D. Tang, Y. Zha, Y. Shi, S. Tu, *J. Heterocycl. Chem.* **2011**, *48*, 957–960.

[33] M. J. Hour, L. J. Huang, S. C. Kuo, Y. Xia, K. Bastow, Y. Nakanishi, E. Hamel, K. H. Lee, *J. Med. Chem.* **2000**, *43*, 4479–4487.

[34] A. B. Bhat, D. P. Sahu, *Synth. Commun.* **2004**, *34*, 2169–2176.

[35] L. Y. Zeng, C. Cai, *J. Heterocycl. Chem.* **2010**, *47*, 1035–1039.

[36] P. R. Bhalla, B. L. Walworth, (American Cyanamid Co., Stanford, CT, USA) EP 0058822 A1, **1982**. [*Chem. Abstr.* **1983**, *98*, 1669].

[37] J. J. Caldwell, E. J. Welsh, C. Matijssen, V. E. Anderson, L. Antoni, K. Boxall, F. Urban, A. Hayes, F. I. Raynaud, L. J. Rigoreau, T. Raynham, G. W. Aherne, L. H. Pearl, A. W. Oliver, M. D. Garrett, I. Collins, *J. Med. Chem.* **2011**, *54*, 580–590.

[38] T. G. Deligeorgiev, S. Kaloyanova, A. Vasilev, J. J. Vaquero, J. Alvarez-Builla, A. M. Cuadro, *Color. Technol.* **2010**, *126*, 24–30.

[39] R. Zink, I. J. Fletcher, (Ciba-Geigy AG, Basel, Switzerland) EP 0109930 A1, **1984** [*Chem. Abstr.* **1984**, *101*, 181249].

[40] R. L. McKee, M. K. McKee, R. W. Bost, *J. Am. Chem. Soc.* **1947**, *69*, 940–942.

[41] S. Lühr, M. Vilches-Herrera, A. Fierro, R. R. Ramsay, D. E. Edmondson, M. Reyes-Parada, B. K. Cassels, P. Iturriaga-Vásquez, *Bioorg. Med. Chem.* **2010**, *18*, 1388–1395.

[42] G. Solladié, Y. Pasturel-Jacopé, J. Maignan, *Tetrahedron* **2003**, *59*, 3315–3321.

[43] E. Schipper, M. Cinnamon, L. Rascher, Y. H. Chiang, W. Oroshnik, *Tetrahedron Lett.* **1968**, *9*, 6201–6204.

[44] J. Hanusek, L. Hejtmánková, L. Kubicová, M. Sedlák, *Molecules* **2001**, *6*, 323–337.

[45] A. Bartolozzi, S. Campbell, B. Cole, J. Ellis, H. Foudoulakis, B. Kirk, S. Ram, P. Sweetnam, M. Hauer-Jensen, M. Boerma, (Surface Logix, Inc., Brighton, MA, USA) Int. PCT Pub. No. WO 2008/054599 A3, **2008**; [*Chem. Abstr.* **2008**, *148*, 538292].

[46] A. D. Roy, A. Subramanian, R. Roy, *J. Org. Chem.* **2006**, *71*, 382–385.

[47] V. S. Patel, S. R. Patel, *J. Indian Chem. Soc.* **1968**, *45*, 167–170.

[48] F. Kashanchi, K. Kehn-Hall, *Curr. Pharm. Des.* **2009**, *15*, 2520–2532.

[49] J. Méndez, *Cell* **2003**, *114*, 398–399.

[50] C. Barrière, D. Santamaría, A. Cerqueira, J. Galán, A. Martín, S. Ortega, M. Malumbres, P. Dubus, M. Barbacid, *Mol. Oncol.* **2007**, *1*, 72–83.

[51] S. Nekhai, M. Zhou, A. Fernandez, W. S. Lane, N. J. Lamb, J. Brady, A. Kumar, *Biochem. J.* **2002**, *364*, 649–657.

[52] T. Ammosova, R. Berro, M. Jerebtsova, A. Jackson, S. Charles, Z. Klase, W. Southerland, V. R. Gordeuk, F. Kashanchi, S. Nekhai, *Retrovirology* **2006**, *3*, 78.

[53] D. Breuer, A. Kotelkin, T. Ammosova, N. Kumari, A. Ivanov, A. V. Ilatovskiy, M. Beullens, P. R. Roane, M. Bollen, M. G. Petukhov, F. Kashanchi, S. Nekhai, *Retrovirology* **2012**, *9*, 94.

[54] S. Baumli, J. A. Endicott, L. N. Johnson, *Chem. Biol.* **2010**, *17*, 931–936.

[55] T. H. Tahirov, N. D. Babayeva, K. Varzavand, J. J. Cooper, S. C. Sedore, D. H. Price, *Nature* **2010**, *465*, 747–751.

[56] S. Wang, G. Griffiths, C. A. Midgley, A. L. Barnett, M. Cooper, J. Grabarek, L. Ingram, W. Jackson, G. Kontopidis, S. J. McClue, C. McInnes, J. McLachlan, C. Meades, M. Mezna, I. Stuart, M. P. Thomas, D. I. Zheleva, D. P.

Lane, R. C. Jackson, D. M. Glover, D. G. Blake, P. M. Fischer, *Chem. Biol.* **2010**, *17*, 1111–1121.

[57] S. Baumli, A. J. Hole, M. E. Noble, J. A. Endicott, *ACS Chem. Biol.* **2012**, *7*, 811–816.

[58] H. Shao, S. Shi, S. Huang, A. J. Hole, A. Y. Abbas, S. Baumli, X. Liu, F. Lam, D. W. Foley, P. M. Fischer, M. Noble, J. A. Endicott, C. Pepper, S. Wang, *J. Med. Chem.* **2013**, *56*, 640–659.

[59] A. J. Hole, S. Baumli, H. Shao, S. Shi, S. Huang, C. Pepper, P. M. Fischer, S. Wang, J. A. Endicott, M. E. Noble, *J. Med. Chem.* **2013**, *56*, 660–670.

[60] L. Sancineto, N. Iraci, S. Massari, O. Tabarrini, *Curr. Med. Chem.* **2013**, *20*, 1355–1381.

[61] Schrödinger Suite 2011, Schrödinger, LLC, New York, NY, **2011**.

[62] Impact version 5.7, Schrödinger, LLC, New York, NY, **2011**.

[63] Prime version 2.3, Schrödinger, LLC, New York, NY, **2011**.

[64] W. L. Jorgensen, D. S. Maxwell, J. Tirado-Rives, *J. Am. Chem. Soc.* **1996**, *118*, 11225–11236.

[65] Glide, version 5.7, Schrödinger, LLC, New York, NY, **2011**.

[66] LigPrep, version 2.5, Schrödinger, LLC, New York, NY, **2011**.

[67] W. C. Still, A. Tempczyk, R. C. Hawley, T. Hendrickson, *J. Am. Chem. Soc.* **1990**, *112*, 6127–6129.

[68] W. L. Jorgensen, J. Tirado-Rives, *J. Comput. Chem.* **2005**, *26*, 1689–1700.

[69] W. L. Jorgensen, L. L. Thomas, *J. Chem. Theory Comput.* **2008**, *4*, 869–876.

[70] W. L. Jorgensen, J. Chandrasekhar, J. D. Madura, R. W. Impey, M. L. J. Klein, *J. Chem. Phys.* **1983**, *79*, 926–935.

[71] W. L. Jorgensen, J. Tirado-Rives, *Proc. Natl. Acad. Sci. USA* **2005**, *102*, 6665–6670.

[72] A. Sabò, M. Lusic, A. Cereseto, M. Giacca, *Mol. Cell. Biol.* **2008**, *28*, 2201–2212.

[73] S. Massari, D. Daelemans, M. L. Barreca, A. Knezevich, S. Sabatini, V. Cecchetti, A. Marcello, C. Pannecouque, O. Tabarrini, *J. Med. Chem.* **2010**, *53*, 641–648.

[74] A. Marcello, P. Massimi, L. Banks, M. Giacca, *J. Virol.* **2000**, *74*, 9090–9098.

[75] P. Pevarello, M. G. Brasca, R. Amici, P. Orsini, G. Traquandi, L. Corti, C. Piutti, P. Sansonna, M. Villa, B. S. Pierce, M. Pulici, P. Giordano, K. Martina, E. L. Fritzen, R. A. Nugent, E. Casale, A. Cameron, M. Ciomei, F. Roletto, A. Isacchi, G. Fogliatto, E.; Pesenti, W. Pastori, A. Marsiglio, K. L. Leach, P. M. Clare, F. Fiorentini, M. Varasi, A. Vulpetti, M. A. Warpehoski, *J. Med. Chem.* **2004**, *47*, 3367–3380; E. Pesenti, W. Pastori, A. Marsiglio, K. L. Leach, P. M. Clare, F. Fiorentini, M. Varasi, A. Vulpetti, M. A. Warpehoski, *J. Med. Chem.* **2004**, *47*, 3367–3380.

[76] R. Pauwels, J. Balzarini, M. Baba, R. Snoeck, D. Schols, P. Herdewijn, J. Desmyter, E. De Clercq, *J. Virol. Methods* **1988**, *20*, 309–321.

[77] C. Pannecouque, D. Daelemans, E. De Clercq, *Nat. Protoc.* **2008**, *3*, 427–434.

[78] M. Popovic, M. G. Sarngadharan, E. Read, R. C. Gallo, *Science* **1984**, *224*, 497–500.

[79] H. Miyoshi, I. Taguchi, S. Kobonishi, Y. Yoshimoto, Y. Ohtsuki, T. Shiraishi, T. Akagi, *Gann Monogr.* **1982**, *28*, 219–228.

[80] The PyMOL Molecular Graphics System, Version 1.5.0.4 Schrödinger, LLC.